

Fiber-optic detection of nitroaromatic explosives with solution-processable triazatruxene-based hyperbranched conjugated polymer nanoparticles

Yuxiang Xu,^{ab} Xiaofu Wu,^a Yonghong Chen,^{ab} Hao Hang,^{ab} Hui Tong^{a*} and Lixiang Wang^{a*}

^aState Key Laboratory of Polymer Physics and Chemistry, Changchun Institute of Applied Chemistry, Chinese Academy of Sciences, Changchun 130022, P. R. China.

^bUniversity of Chinese Academy of Sciences, Beijing 100049, P. R. China.

E-mail: chemtonghui@ciac.ac.cn; lixiang@ciac.ac.cn.

Supporting Information

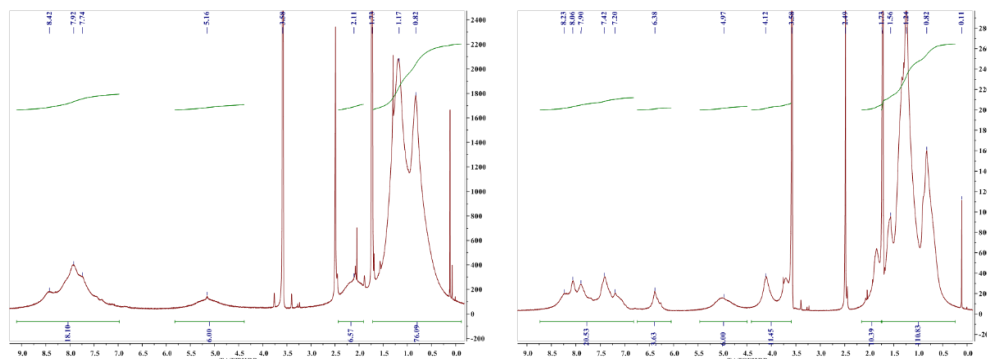


Fig. S1. ¹H NMR spectra of TATF8HBP (left) and TATSFHBP (right) in THF-d8.

Table S1. Elemental content of TATF8HBP and TATSFHBP.

Polymer		C	H	N	O
TATF8HBP	Calc.	87.19%	9.24%	3.57%	-
	Anal.	84.55%	9.37%	3.61%	-
TATSFHBP	Calc.	83.42%	9.06%	2.29%	5.23%
	Anal.	82.72%	9.55%	2.33%	n.d.

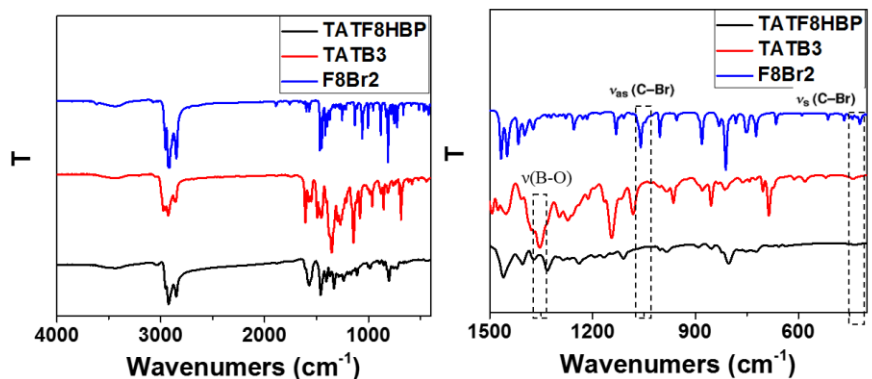


Fig. S2. FT-IR spectra of **TATF8HBP**, **TATB3** and **F8Br2**.

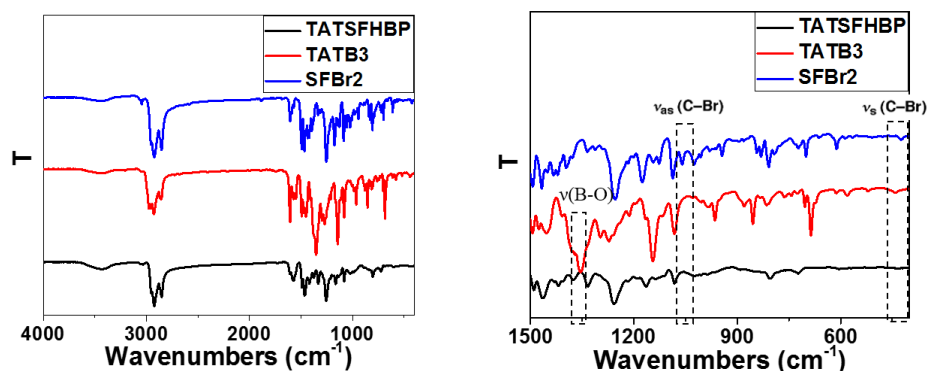


Fig. S3. FT-IR spectra of **TATSFHBP**, **TATB3** and **SFBr2**.

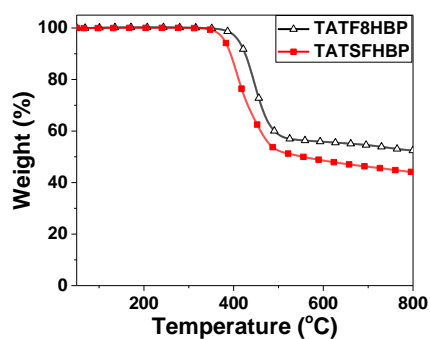


Fig. S4. TGA curves of **TATF8HBP** and **TATSFHBP** recorded under N₂ atmosphere.

Table S2. Physical properties of **TATF8HBP** and **TATSFHBP**.

Polymer	$\lambda_{\text{abs}}[\text{nm}]$		$\lambda_{\text{em}}[\text{nm}]$		QY		T_d [°C]	E_g^{opt} [eV]	E_{HOMO}^c [eV]	E_{LUMO}^d [eV]
	sol.	film	sol.	film	sol. ^a	film ^b				
TATF8HBP	385	385	443	470	34.2%	5.3%	411	2.85	-5.12	-2.27
TATSFHBP	392	392	445	462	58.3%	14.7%	380	2.80	-5.12	-2.32

^aIn dilute THF, using 9,10-Diphenylanthracene in cyclohexene as standard. ^bMeasured by the integrating sphere. ^c $E_{\text{HOMO}}=-(E_{\text{ox}}-E_{\text{ox},\text{Fc}})-4.8$ eV. ^d $E_{\text{LUMO}}=E_g^{\text{opt}}+E_{\text{HOMO}}$.



Fig. S5. Images of **TATF8HBP** and **TATSFHBP** films coated on quartz plates.

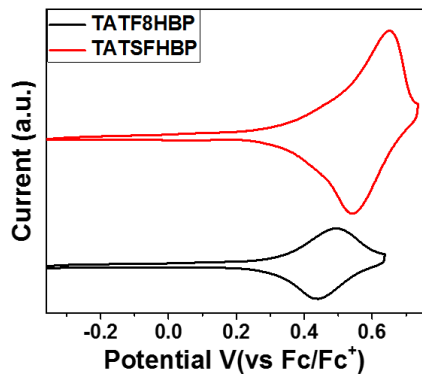


Fig. S6. Cyclic voltammograms of **TATF8HBP** and **TATSFHBP** in thin films measured in acetonitrile with TBAPF₆ as supporting electrolyte.

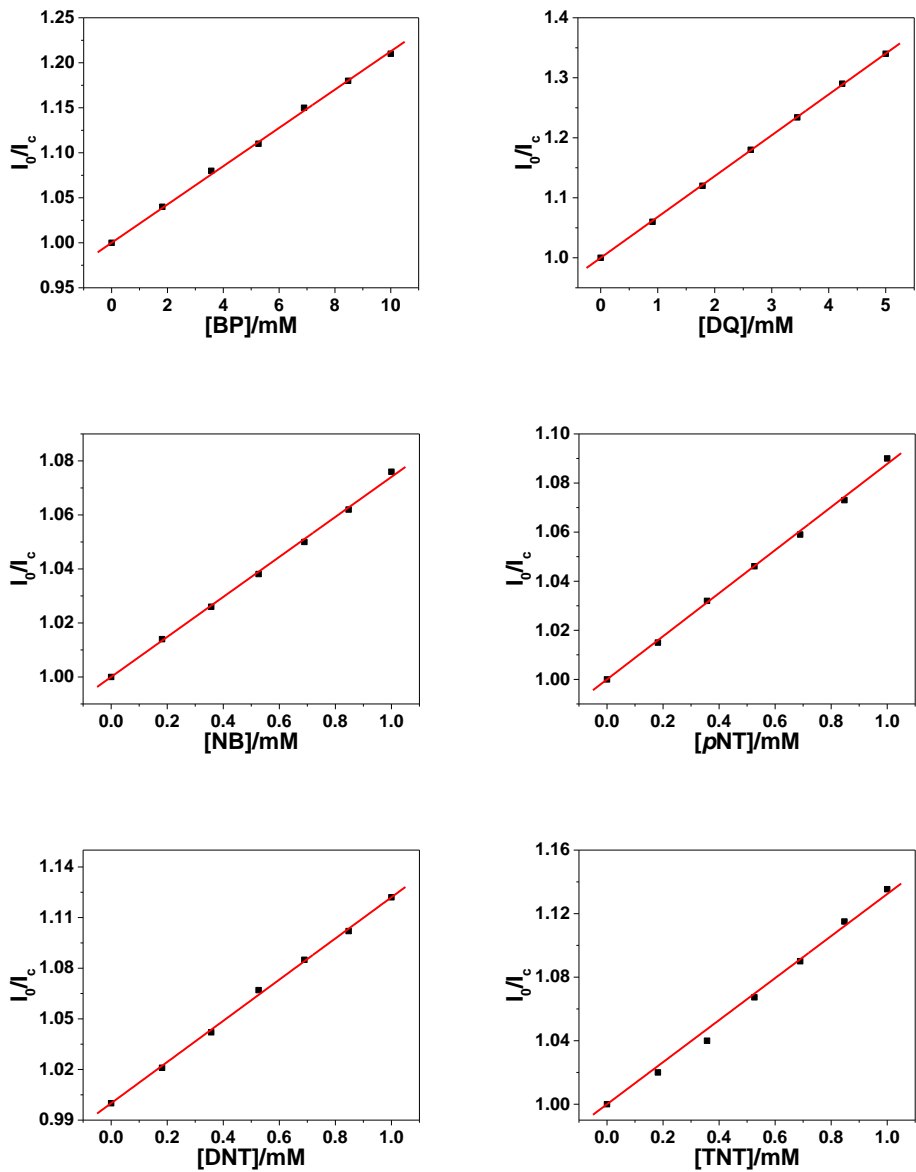


Fig. S7. Stern-Volmer plots and fits for **TATF8HBP** with the six different analytes.

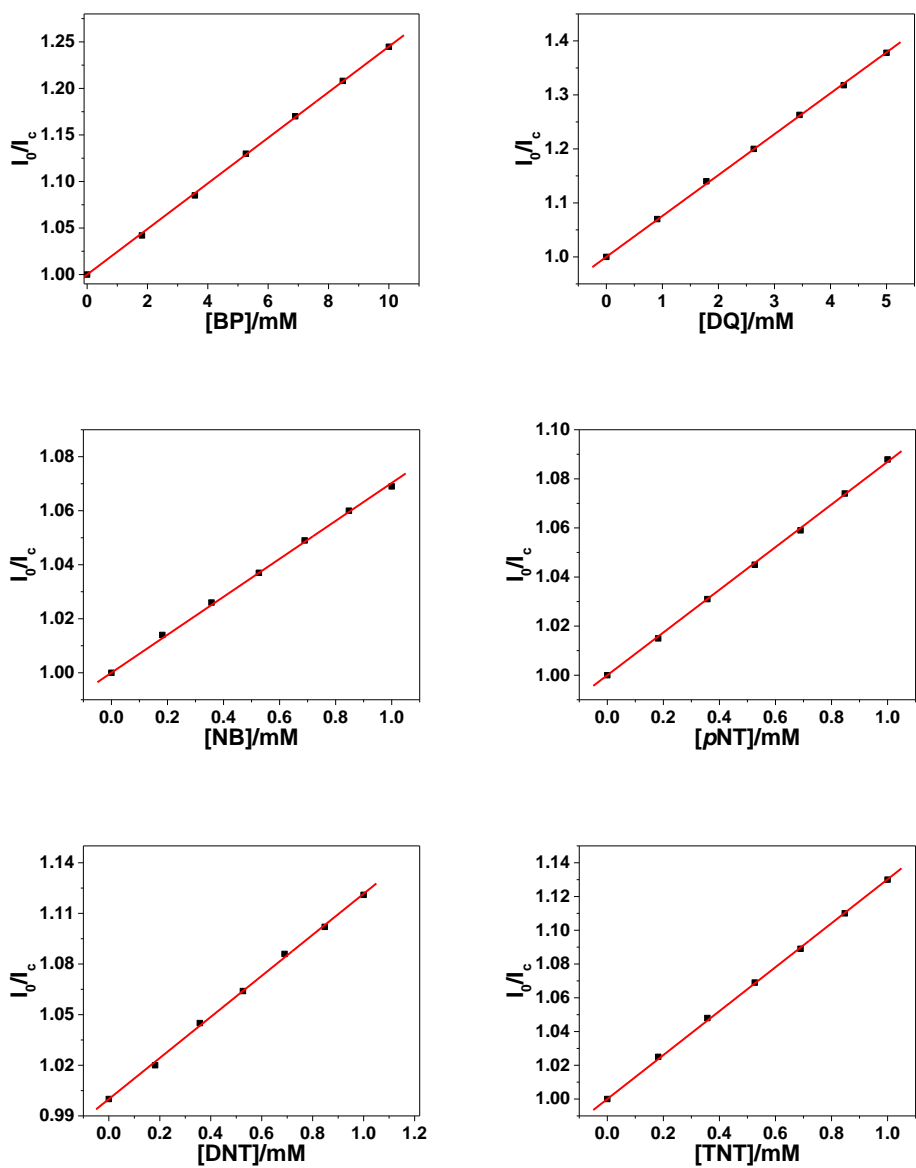


Fig. S8. Stern-Volmer plots and fits for **TATSFHBP** with the six different analytes.

Table S3. Summary of the Stern-Volmer Constants (K_{sv}) for each polymers with different analytes.

Polymer	TNT/ M^{-1}	DNT/ M^{-1}	p NT/ M^{-1}	NB/ M^{-1}	DQ/ M^{-1}	BP/ M^{-1}
TATF8HBP	132.3 ± 2.4	122.0 ± 1.0	87.8 ± 0.8	74.1 ± 0.7	68.1 ± 0.2	21.3 ± 0.2
TATSFHBP	130.2 ± 0.5	121.7 ± 0.9	86.9 ± 0.4	70.3 ± 0.5	75.8 ± 0.3	24.5 ± 0.1

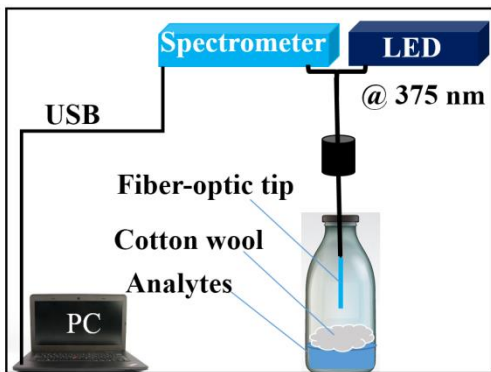


Fig. S9. A schematic drawing of an experimental setup for fiber-optic sensing of explosive vapors.

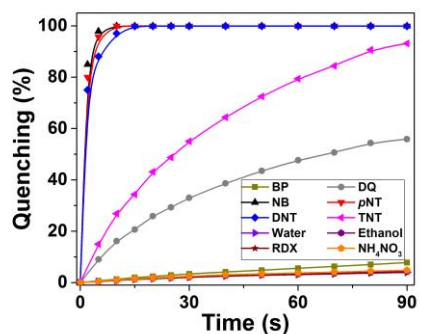


Fig. S10. Time-dependent fluorescence quenching of **TATSFHBP** films coated on fiber-optic tips upon exposure to saturated DNT, TNT, *p*NT, NB, DQ, BP, ethanol, water, RDX and NH₄NO₃ vapors.

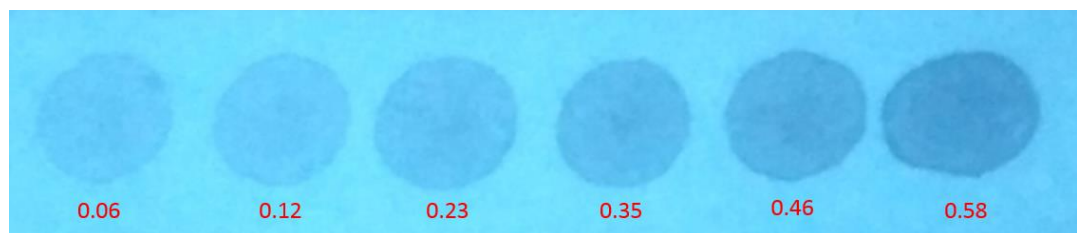


Fig. S11. Fluorescence quenching images of TNT-indicating papers quenched by TNT with various amounts (unit: ng·mm⁻²).